

# Difference in Steady Shear Flow Viscosity between Polar and Nonpolar Nematic Liquid Crystals in Aromatic Polyesters Derived from VECTRA

Yoshiaki Taguchi,<sup>†,‡</sup> Chu-Chun Yen,<sup>†</sup> Sungmin Kang,<sup>†</sup> Masatoshi Tokita,<sup>†</sup> and Junji Watanabe<sup>\*,†</sup>

Department of Organic and Polymeric Materials, Tokyo Institute of Technology, Ookayama, Meguro-ku, Tokyo 152-8552, Japan, and Research and Develop Center, Polyplastics Co., Ltd., 973, Miyajima, Fuji, Shizuoka 416-8533, Japan

Received December 8, 2008; Revised Manuscript Received March 3, 2009

**ABSTRACT:** Steady shear flow viscosities were measured for nematic liquid crystals (LCs) in the aromatic copolyesters composed of 4-hydroxybenzoic acid (HBA), 6-hydroxy-2-naphthoic acid (HNA), terephthalic acid, and biphenol whose molar contents are  $0.73 - x$ ,  $0.27 - x$ ,  $x$ , and  $x$ , respectively. Second harmonic generation (SHG) measurements showed that a SHG-active polar nematic LC formed by poly(HBA/HNA) with  $x = 0$  is altered to a conventional nonpolar nematic LC with an increase in  $x$  more than 0.07. The shear-rate dependence of melt viscosity measured for nematic LCs of all the copolymers showed four characteristic regions; a Newtonian plateau in lowest shear-rate region 0 in addition to the well-known three regions, low-shear-rate shear-thinning region I, intermediate Newtonian plateau region II and high-shear-rate shear-thinning region III. The SHG-activity in nematic LCs reflected on the Newtonian plateau region 0. The viscosity of the SHG-active nematic LCs in this region 0 was 10 times higher than that of the non-SHG-active nematic ones. The higher viscosity of the SHG-active nematic LC was connected to the smaller domain size (or larger number of disclinations) estimated by small-angle light scattering. In the nonpolar nematic LC, many disclinations initially formed were easily annihilated because of a coalescence of two disclinations with opposite signs, whereas in the polar nematic LC, such an annihilation hardly occurred because of the polar packing symmetry.

## 1. Introduction

Aromatic polyesters are most important class of thermotropic liquid crystal (LC) polymers. They show outstanding physical properties and excellent chemical resistance suitable for commercial applications in electronics, automotive and aerospace industries as well as in medical fields.<sup>1</sup> Typical thermotropic LC polyester is a copolymer composed of 4-hydroxybenzoic acid (HBA) and 6-hydroxy-2-naphthoic acid (HNA). Random incorporation of HNA units into poly(HBA) decreases the melting point to 250 °C and makes the nematic LC phase thermally accessible.<sup>2</sup> It was first commercialized in 1985 as the VECTRA series of moldable LC polymers. Typical poly-(HBA/HNA), called as VECTRA A950, is composed of 73 mol % of HBA and 27 mol % of HNA.

VECTRA polyester is an extraordinary class of LC polymers, since a head-to-tail connection of HBA and HNA<sup>3–5</sup> results in a large dipole moment along the chain as a result of accumulation of the carbonyl dipole in ester linkage.<sup>6</sup> Because of such a polar rod-like conformation, poly(HBA/HNA) can form the polar nematic LC, which has been experimentally confirmed by second harmonic generation (SHG) measurements<sup>7–11</sup> and predicted by computer simulation and theoretical calculation considering the dipole–dipole interaction.<sup>12–15</sup> Another interesting aspect of nematic LC of poly(HBA/HNA) is observed on the shear-flow behavior. It shows very high shear-flow viscosity of around  $10^3$  Pa·s at shear rates lower than  $10^{-2}$  s<sup>-1</sup> while the conventional nematic LC in other commercialized polyesters show the viscosity of around  $10^2$  Pa·s.<sup>16,17</sup> These two characteristics, SHG-active polar nematic structure and high viscosity at low shear rates, seem to be significantly related to each other.

As reported in a previous paper,<sup>8</sup> the head–tail character in poly(HBA/HNA), can be eliminated by introduction of symmetrical units of terephthalic acid (TA) and biphenol (BP) which cancels the dipole moments along the chain axis within a polymer chain. We have thus prepared an interesting series

**Table 1. Characterization of the Copolyesters**

sample	mole fraction of TA unit	$\eta_{inh}/dL\ g^{-1}$	$T_m/^\circ C^a$	relative SHG intensity	$D/\mu m$
P-Std	0	4.67	283	1.00	5.3
P-0.003	0.003	3.46	283	0.78	4.6
P-0.006	0.006	3.91	280	0.63	6.8
P-0.015	0.015	4.26	278	0.42	6.3
P-0.03	0.03	4.38	277	0.05	5.6
P-0.05	0.05	4.23	273	0.03	5.3
P-0.07	0.07	4.14	251	0.00	>10
P-0.08	0.08	3.36	248	0.00	>10
P-0.09	0.09	4.17	248	0.00	>10
P-0.10	0.10	4.31	219	0.00	>10

<sup>a</sup> Based on heating DSC data.

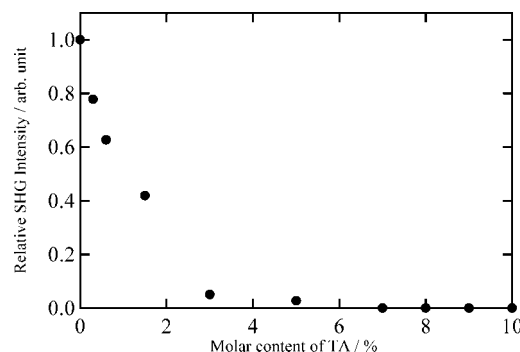


**Figure 1.** Variation of SHG intensity with the mole fraction of TA (or BP) unit in a series of P- $x$  copolyesters. Here, the relative SHG intensity is evaluated as a standard of P-Std.

\* Corresponding author. E-mail: jwatanab@polymer.titech.ac.jp.

<sup>†</sup> Department of Organic and Polymeric Materials, Tokyo Institute of Technology.

<sup>‡</sup> Research and Develop Center, Polyplastics Co., Ltd.

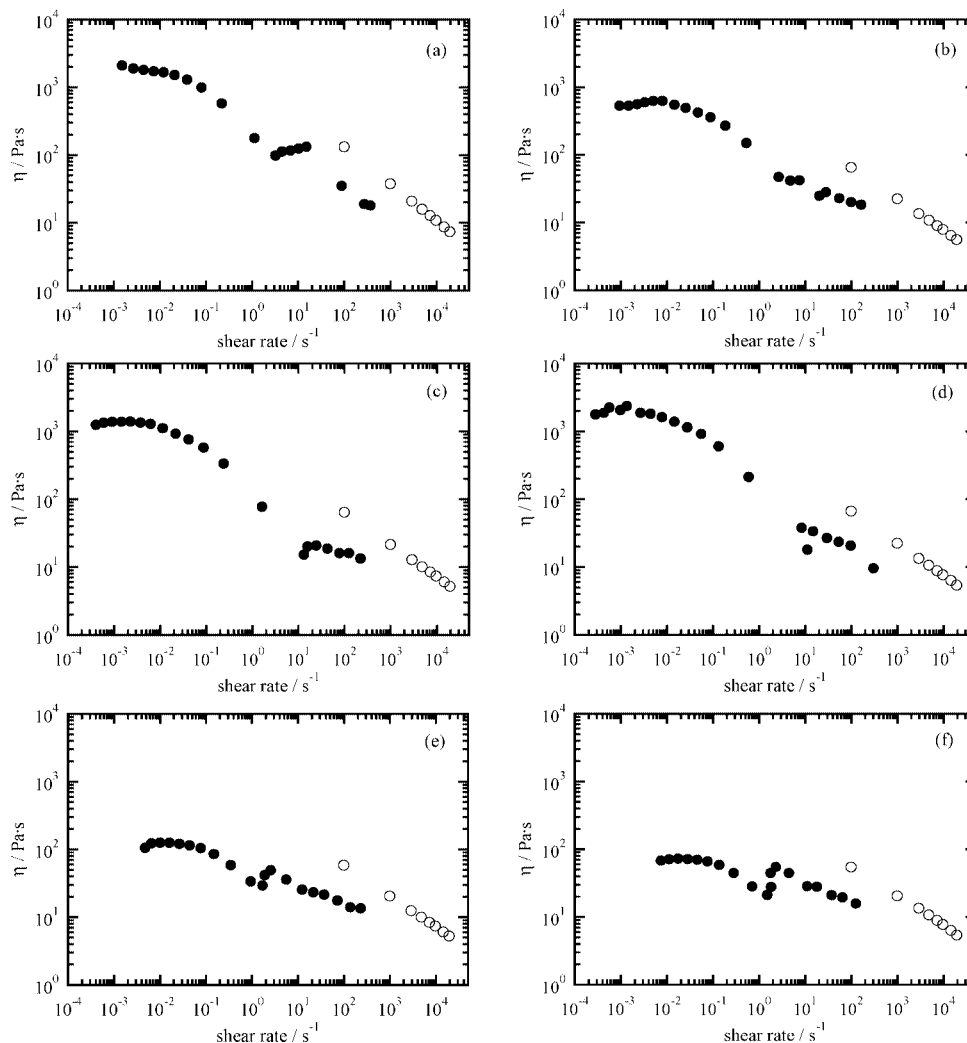


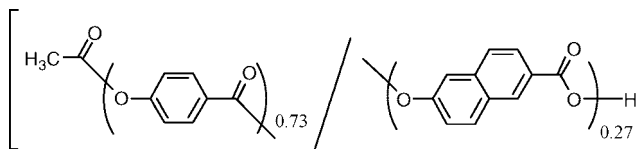
**Figure 2.** Steady-state viscosity for the nematic LCs of (a) P-Std, (b) P-0.015, (c) P-0.03, (d) P-0.05, (e) P-0.07, (f) P-0.09 at 330 °C. The data presented by closed and open circles are collected by the plate-and-plate rheometer and the capillary rheometer, respectively.

of poly(HBA/HNA/TA/BP) polyesters, in which the SHG active and nonactive nematic LCs are formed depending on the content of TA and BP. By using this series of polyesters, in this study, we observed carefully the steady shear flow viscosity of the nematic LCs in a wide shear-rate range from  $10^{-3}$  to  $10^4$   $\text{s}^{-1}$  and obtained the well-defined viscosity curves which include a Newtonian plateau in lowest shear rate region (region 0) in addition to the well-known three regions I, II, and III characteristic to the LC polymers.<sup>18</sup> The result indicates that the viscosity in region 0 strongly depends on whether the nematic LC is SHG-active or not whereas the viscosities in regions II and III do not. The viscosity of the SHG active nematic LC in region 0 is 10 times higher than that of the SHG nonactive ones. This difference in the viscosity of region 0 can be definitely connected to the difference in the domain size (or the number of defects) which is attributed to the difference in the annihilation modes of defects between polar and nonpolar nematic LCs.

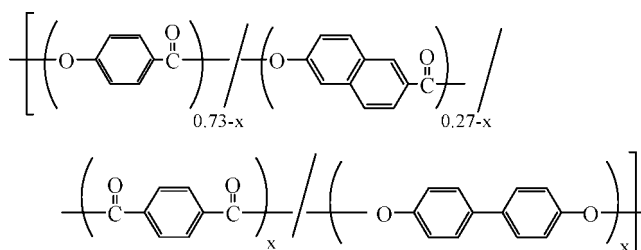
## 2. Experimental Section

**2.1. Materials.** VECTRA A950 comprised of HBA and HNA units with a molar ratio of 73/27, which is commercially available, was supplied by Polyplastics Co. Ltd. The weight-averaged molecular weight ( $M_w$ ) and the polydispersity of the molecular weight of VECTRA A950 have been estimated to be 30000,<sup>19</sup> and

2.45,<sup>20</sup> respectively. In this study, VECTRA A950 is treated as a standard polymer, and abbreviated here as P-Std.



The copolymers in which terephthalic acid (TA) and biphenol (BP) units were incorporated into VECTRA A950 were synthesized by the method according to the applied patent from Celanese.<sup>21</sup> The content of TA or BP that should be equimolar with each other in order to properly perform the polymerization, was varied from 0 to 0.1. These copolymers with the following structure are designated as P- $x$  where  $x$  is the molar content of TA or BP unit.



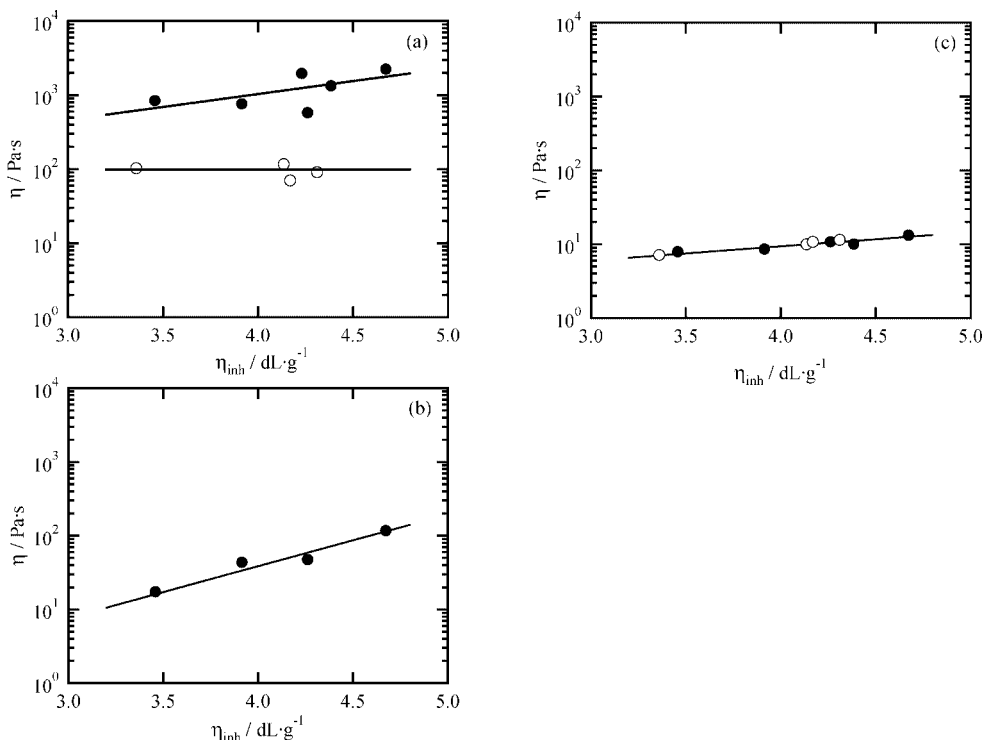


**Figure 3.** Variation of apparent viscosity (a) in the lowest-shear-rate Newtonian plateau (region 0), (b) in the high-shear-rate Newtonian plateau (region II), and (c) at a shear rate of  $4864 \text{ s}^{-1}$  in high-shear-rate shear-thinning region III with inherent viscosity of copolymers. The applied temperature is  $330^\circ\text{C}$ . The viscosities of the SHG-active and non-SHG-active polymers are plotted by closed and open symbols, respectively.

Inherent viscosities,  $\eta_{\text{inh}}$ , and crystal–nematic LC transition temperatures,  $T_m$ , of these polymers are listed in third and forth columns in Table 1, respectively. Here,  $\eta_{\text{inh}}$  of the polymers were measured for solutions of the equivolume mixture of pentafluoro phenol (PFP) and hexafluoro isopropanol at a concentration of  $0.1 \text{ g dL}^{-1}$  at  $30^\circ\text{C}$ , and  $T_m$  was determined by differential scanning calorimetry (DSC) on heating at a rate of  $20^\circ\text{C min}^{-1}$  (TA Instruments DSC Q-1000). At temperatures higher than  $T_m$ , all of the polymers were confirmed to form the nematic phase by polarized optical microscopy (Olympus BX 51 equipped with a Mettler FP82HT hotstage) and wide-angle X-ray diffraction (Cu K $\alpha$  radiation, Rigaku UltraX18 generator equipped with the hotstage). No nematic to isotropic phase transition was observed in a temperature region up to  $350^\circ\text{C}$ .

**2.2. Methods. SHG Measurement.** SHG was used as a probe to monitor the spontaneous polarization in the medium.  $\text{Q-switched Nd:YAG}$  laser generated with a HOYA Continuum SL-II with the pulse energy of  $0.4 \text{ mJ cm}^{-2}$ . The laser pulse width and the repetition frequency were  $8 \text{ ns}$  and  $10 \text{ Hz}$ , respectively. The fundamental laser beam was incident perpendicular to thin films with thickness of  $\sim 10 \mu\text{m}$  (illumination area;  $0.1 \text{ mm}$  in diameter) after passing through a quarter-wave plate and a polarizer. SH light ( $\lambda = 532 \text{ nm}$ ) generated was detected by a Hamamatsu model-R955 photomultiplier tube in a transmitted direction after passing through an IR cut filter, an interference filter and an analyzer. The electronically converted signals of the SH light were accumulated in a Stanford Research System BOXCAR integrator and output to a personal computer.

The oriented films with thickness of  $\sim 10 \mu\text{m}$  were prepared by drawing out from a slit die ( $5 \text{ mm}$  in wide,  $1 \text{ mm}$  in length and  $10 \text{ mm}$  in height) at a rate of  $100 \text{ mm min}^{-1}$  and pressed at  $330^\circ\text{C}$ . SHG measurements were performed with both the polarizer and analyzer set parallel to the orientation (polymer chain) axis.<sup>7</sup> Relative SHG intensities for all the P- $x$  polymers were determined as a standard of P-Std by a contact method where the P- $x$  film was contacted with the P-Std film and the SH signal intensity was detected by scanning the laser beam

from the area of one polymer to that of the other.<sup>7,8</sup> The values thus determined are listed in the fifth column of Table 1.

**Viscosity Measurement.** Steady flow viscosity measurements were performed with a Rheometric SR200 equipped with parallel plate configuration with  $12.5 \text{ mm}$  in radius ( $R$ ) and  $1.5 \text{ mm}$  in gap ( $H$ ) under nitrogen atmosphere. Shear rate  $\dot{\gamma}$  is calculated by  $\dot{\gamma} = (2\pi/60)(R/H)n$  where  $n$  is the rotational speed of the plate ( $\text{min}^{-1}$ ). To avoid structural changes due to a squeezing flow on loading the sample,<sup>23</sup> powdered samples with the size of a few micrometers were first prepared from pellets and pressed into disk-like form under a vacuum without heating. The disk-like sample was then set between the parallel plates, heated up to  $330^\circ\text{C}$ , and annealed for  $10 \text{ min}$ . At first, the sample was sheared at the lowest shear rate of  $10^{-3} \text{ s}^{-1}$ . After confirming that the viscosity value is not changed in the time span of  $5$  to  $10 \text{ min}$ , we measured the viscosities with increasing the shear rate up to  $10^2 \text{ s}^{-1}$ . The temperature of  $330^\circ\text{C}$  was selected to avoid the crystallization of the sample during measurements, which are completed within  $30 \text{ min}$ .

Capillary flow measurements were performed at  $330^\circ\text{C}$  with a Toyo Seiki CAPILLOGRAPH 1B with a capillary with  $0.5 \text{ mm}$  in diameter and  $30 \text{ mm}$  in length having a flat entrance angle. Shear rates were varied from  $10^2$  to  $10^4 \text{ s}^{-1}$ .

**Light Scattering Measurement.** Small-angle light scattering patterns were measured by using an Otsuka electric DYNA-3000. Here, the polymers were dissolved in  $50/50 \text{ v/v}$  mixture of PFP and chloroform, and cast on a slide glass. The film with a thickness of  $\sim 10 \mu\text{m}$  was then rinsed with chloroform and dried under vacuum at  $80^\circ\text{C}$ . The scattering patterns were recorded after annealing the film in nematic LC at  $330^\circ\text{C}$  for  $30 \text{ min}$ .

### 3. Results and Discussion

**3.1. Alteration of SHG-Active to Non SHG-Active Nematic LC by Introducing Symmetrical Comonomer Units into P-Std.** P- $x$  polymer chain loses the head–tail nature by an introduction of symmetric BP and TA units so that the resulting nematic LC loses the polarity as well.<sup>8</sup> This trend is clearly observed in fifth column of Table 1, and in Figure 1

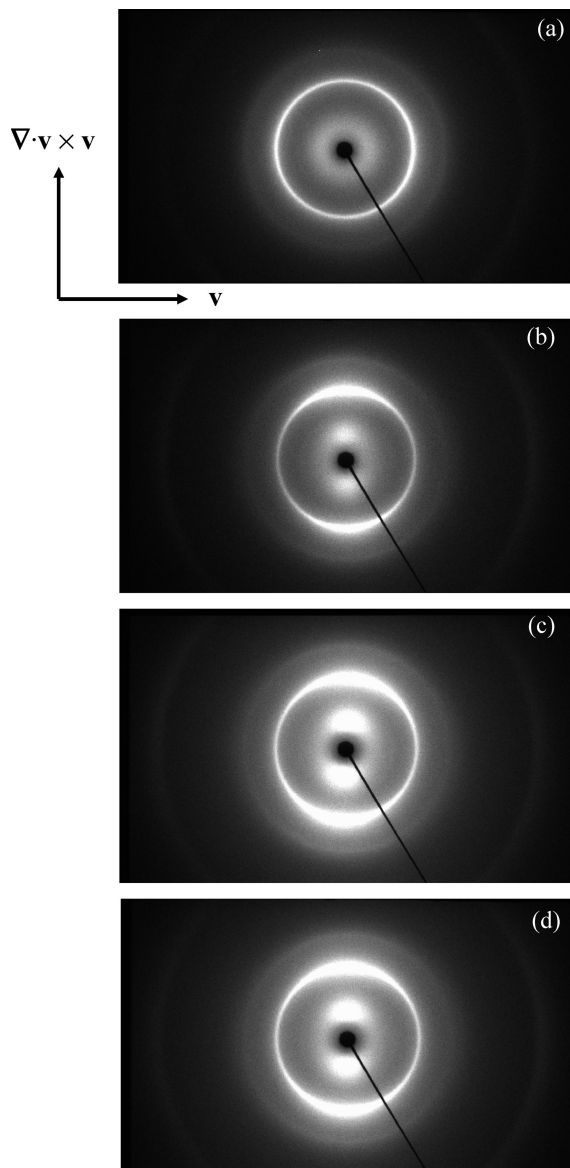


**Figure 4.** WAXD patterns of P-Std nematic film sheared by rotational rheometer in regions (a) 0, (b) I, (c) II, and (d) III. X-ray beam was irradiated along the velocity gradient ( $\nabla \mathbf{v}$ ) direction. The strong reflection in the central part has a spacing of 4.8 Å, which is attributed to the lateral packing of polymers.

where the relative SHG of the nematic LCs in P-*x* is plotted against the content *x* of TA (or BP). SHG intensity sharply decreases with increasing *x* and becomes zero for P-*x* with *x* more than 0.07, indicating that the perfect alteration from the polar nematic LC to the nonpolar (or conventional) one is accomplished on increasing *x* up to 0.07.

The critical TA fraction of 0.07 is slightly larger than that of 0.05 reported in a previous paper,<sup>8</sup> but this can be explained by the difference in SHG measurement set up. In the previous work,<sup>8</sup> the laser was irradiated on nonoriented samples while in this work it was irradiated on the oriented samples with the measurement geometry set to detect the maximum SHG signal. The values determined in this work seem more accurate than that in the previous one.

**3.2. Steady Shear Flow Viscosity.** Steady shear flow viscosities for nematic LCs of all the prepared polymers were measured at 330 °C by a parallel-plate type of rheometer in a wide shear-rate range from  $10^{-3}$  to  $10^2$  s<sup>-1</sup>. Typical viscosity data (closed circles) are shown in Figure 2a–f. The viscosities

were also measured by the capillary rheometer in high shear rate zone from  $10^2$  to  $10^4$  s<sup>-1</sup> as shown by open circles. Both methods give the similar shear rate dependences of viscosity. Although the viscosity by the capillary rheometer is relatively larger than that of the rotation rheometer, both values do not need to be equal.

The flow-viscosity curve is well divided into four regions; a Newtonian plateau at the lowest shear-rate regime in addition to three regions which have been well elucidated in LC polymers.<sup>18</sup> Typical example is observed for P-Std in Figure 2a. On increasing the shear rate ( $\dot{\gamma}$ ), the viscosity takes a constant value at  $\dot{\gamma}$  up to  $10^{-1}$  s<sup>-1</sup> (region 0), and then decreases to one-tenth at  $\dot{\gamma}$  from  $10^{-1}$  to  $10^0$  s<sup>-1</sup> (region I). With further increase of the shear rate, the viscosity becomes almost constant in a shear-rate region of  $5 \times 10^0$  to  $5 \times 10^1$  s<sup>-1</sup> (region II), and then decreases again at  $\dot{\gamma}$  larger than  $10^2$  s<sup>-1</sup> (region III). Three of these four flow regions, namely regions I, II and III, are designated to keep a correspondence with those defined by Onogi and Asada,<sup>18</sup> and frequently observed in various polymeric LCs. In contrast, the region 0 is rarely observed. Only the observation of region 0 has been reported in a lyotropic LC of hydroxypropyl cellulose/water system.<sup>24</sup> As far as we know, this is the first clear observation of region 0 in thermotropic LC system. All the samples show the similar behavior although the region II becomes narrower or sometimes disappears as *x* increases more than 0.03 as found in Figure 2d–f.

In Figure 3, the viscosities in respective regions of 0, II and III are plotted as a function of  $\eta_{\text{inh}}$  of polymer. Here, the viscosity measured by the capillary rheometer at a shear rate of 4846 s<sup>-1</sup> was adopted as the viscosity in region III. The viscosity in region II was determined for only four samples because region II becomes unclear on increasing TA or BP fraction as mentioned above. The viscosities in regions II and III show a simple positive correlation with  $\eta_{\text{inh}}$  of polymer, i.e. the molecular weight (see Figure 3b,c). The viscosity in region 0 as shown in Figure 3a, however, depends not only on  $\eta_{\text{inh}}$ , but also on whether the copolyester is SHG-active or not; the viscosities of the six SHG-active copolyesters are around  $10^3$  Pa·s, which is ten times larger than those of the four non-SHG-active copolyesters.

#### 4. Discussion

First interesting result in this study is that the four characteristic regions were well established in the steady shear flow viscosities of polymeric nematic LCs. In other words, there are four different shear flow mechanisms. Here, it should be emphasized that the shear has been applied for the polydomain nematic LC the domain size of which is dominated by the number of disclinations.

Previous works<sup>18,23–25</sup> have shown that in such polydomain LCs the regions I, II, and III have been clearly observed and associated with deformation of LC structures. Two shear-thinning regions I and III separated by intermediate plateau region II are due to the presence of two largely different characteristic times in deformation modes. The shear thinning in the lower shear-rate region I is attributed to the long-range-order elastic deformation of disclinations in polydomain LC whereas the other in highest shear-rate region III is connected to molecular dynamics, the short-range-order elastic deformation of molecular order which produces a uniform molecular orientation.<sup>26</sup> From X-ray patterns taken in respective regions in Figure 4, in fact, some orientation of molecules along the shear direction is observed in region I, and then orientation in region III becomes more improved although no orientation can be detected in region 0. Newtonian region II may appear as an intermediate region where the characteristic distance between disclinations decreases on increasing shear rate on the one hand,



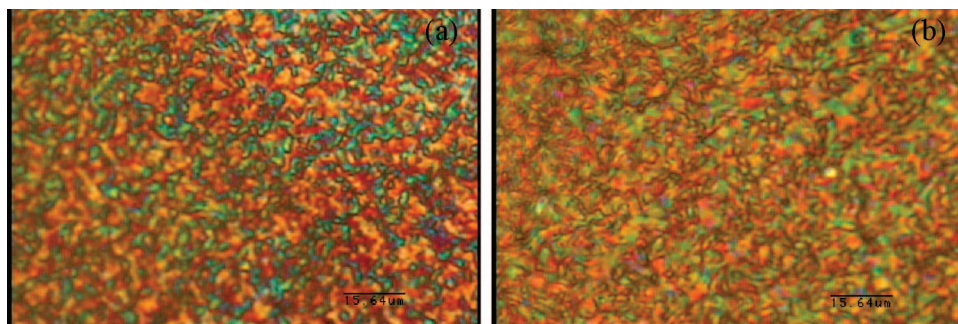


**Figure 5.** Optical microscopic nematic textures of (a) P-Std and (b) P-0.07. The sample thickness is around 10  $\mu\text{m}$ .

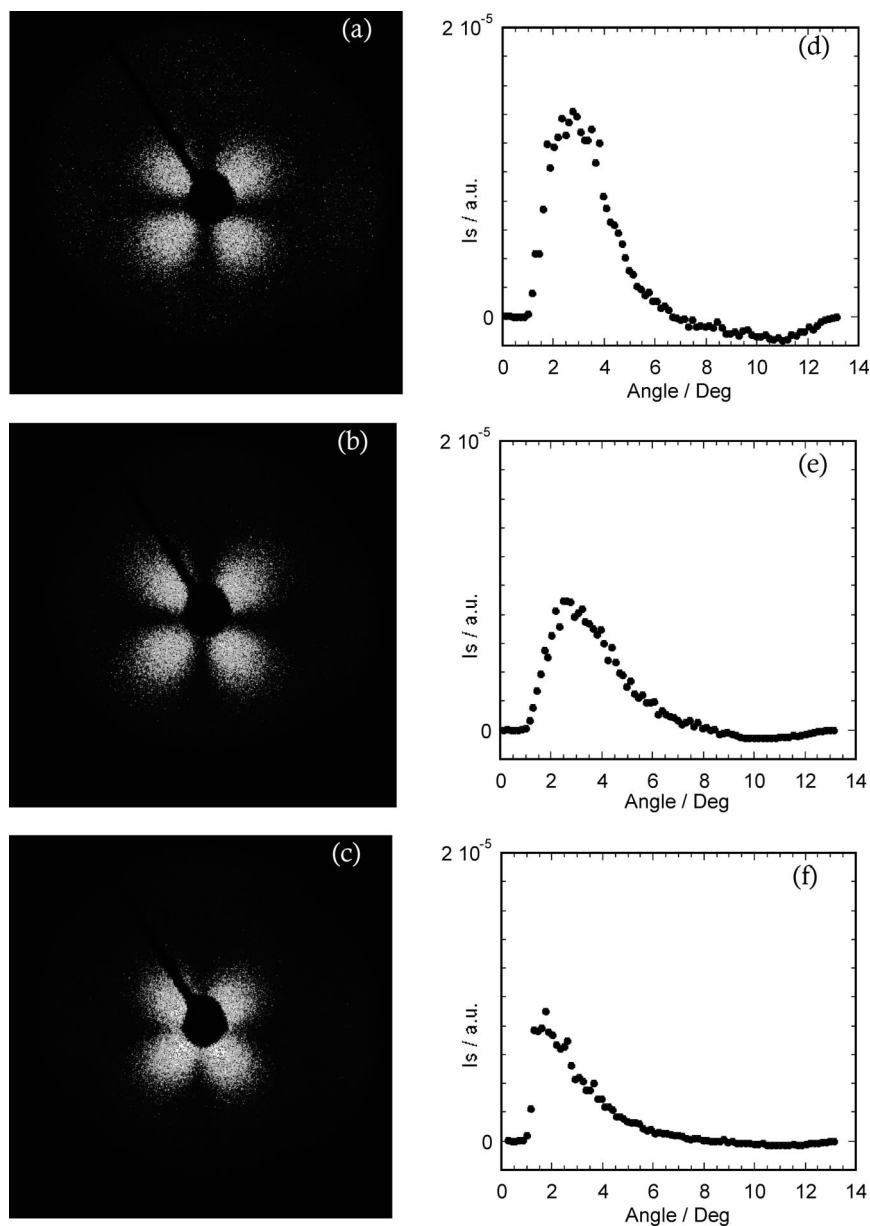


**Figure 6.** (a–c) Small-angle light scattering  $Hv$  pattern and (d–f) its  $2\theta$  intensity profile observed for the nematic LC of (a, d) P-Std, (b, e) P-0.05 and (c, f) P-0.08 at 330  $^{\circ}\text{C}$ .

and the molecules, on the other hand, surely flow. Thus, the three regions I, II and III, are associated with deformation or disturbance of polydomain structure whose length scale is larger with decreasing shear rate.

According to this tendency, the Newtonian plateau appearing in lowest shear-rate region 0 may be associated with flowing

of the domains in such a way that an equilibrium defect density or domain size of the polydomain LC remains constant to a certain extent, which has been theoretically described by Chung et al.<sup>26</sup> by using the Larson-Doi defect density evolution equation<sup>27</sup> with the inclusion of the defect density (number density of disclinations) in the initial polydomain LC. At this

aspect, it is interesting to refer to the second interesting result that the difference in viscosity of region 0 between the SHG active and non SHG-active polymers can be really connected to the domain size difference. By the optical microscopic observations, all of the polymeric nematic LCs at 330 °C show very fine sanded texture where the disclinations and their related Schlierens tend to be very small and blurred, however the relatively large domain can be recognized in the non SHG-active nematic LCs (see Figure 5). The more quantitative analysis for the domain size can be done by small-angle light scattering (SALS) method.<sup>28</sup> The typical SALS patterns are shown in Figure 6a–c. All of the nematic LCs invariantly show a four-leaf SALS pattern but show the different sizes of the pattern which depend on whether the copolymer is SHG active or not. The SHG-active polymers show the scattering patterns expanding into the larger angle region than the non-SHG-active polymers, indicating that in the initial polydomain state just before starting the shear flow viscosity measurement, the domain size (or the distances between disclinations) in the SHG active copolymers is smaller than that in non SHG-active ones. The domain sizes determined from the  $2\theta$ -intensity profile of Figure 6d–f, are listed in six column of Table 1. The domain sizes in the SHG active copolymers are commonly estimated to be about 5  $\mu\text{m}$ , while those in non SHG-active ones are around 10  $\mu\text{m}$  or larger than 10  $\mu\text{m}$ . Such domain sizes can be qualitatively obtained as the distances between the disclinations in microscopic nematic texture in Figure 5. Thus, we conclude that the smaller size domains (i.e., the higher defect densities) in the SHG-active nematic LC are attributed to the

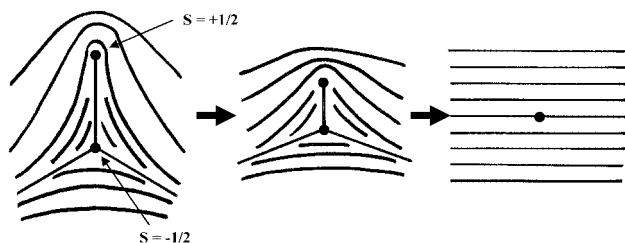


**Figure 7.** Schematic representation of the annihilation microprocess of a pair of  $s = \pm 1/2$  disclinations and the corresponding variations of the schlieren texture with time in conventional nematic phase. Time is prolonged from left illustration to right illustration.

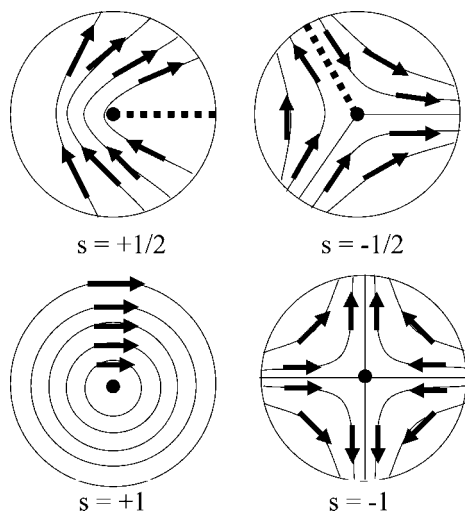


**Figure 8.** Illustration of polar molecules forming the disclinations with  $s = \pm 1/2$  and  $\pm 1$  in polar nematic LC. Arrows indicate the dipole moment vectors. It is found that there is an inconsistency (presented by the dashed line) in alignment of dipole moment vectors in disclinations of  $|s| = 1/2$ .

larger shear-flow viscosity in region 0. This result is interestingly compared with the result obtained for highly concentrated emulsions of the water-in-oil type.<sup>29</sup> In the emulsion system, flow viscosity curves clearly show a low shear-rate Newtonian region, and its viscosity increases with a decrease in droplet size of emulsions which may be equivalent to the domain size in the present system.

Here, we consider the reason why the SHG active nematic LC, i.e. the polar nematic LC,<sup>8,11</sup> possesses the high defect density. Generally, the nematic LC may form many kinds of disclinations with various strengths of  $s = \pm 1/2, \pm 1$  and so on, immediately after the powder samples are heated up to nematic temperature. The sum of the strengths for all disclinations should be zero. In an initial stage on the nematic LC formation, the number of disclinations would be almost same between the polar and nonpolar phases. After a prolonged annealing, however, disclinations of equal and opposite strengths attract one another and are annihilated. One of the examples is shown in Figure 7 which illustrates the topological situation near the center of disclinations of  $|s| = 1/2$  showing how the disclination lines of  $s = +1/2$  and  $s = -1/2$  are annihilated.<sup>31</sup> Thus, many of paired disclinations with opposite signs may disappear altogether or form a new one, leading to the development of the large domain texture with low defect density. Without surface anchoring nor external aligning fields, however, an appreciable number of disclinations are still remained in the pseudoequilibrium state in which size and shape of domain no longer change with time.<sup>30–33</sup>

Such a simple development of domain texture promoted by the director orientation would be unlikely in the case of the polar nematic phase with a low packing symmetry. Figure 8 shows various type of disclinations in nematic LCs. When the dipole moment vectors indicated by the arrows are superimposed on the director curves, we know that the disclination lines or points with  $|s| = 1/2$  are not compatible with the polar structure so that those have to escape into the disclinations with  $|s| = 1$ . Further, neighboring disclinations cannot join each other as occasionally as in the nonpolar phase, but conversely, the new disclinations have to be created with the simultaneous formation of polar structure following the uniaxial alignment of polymers. This may be a reason why the SHG active polar nematic phase possesses the smaller domains than the SHG nonactive one. The detailed examination for the texture development in the polar nematic phase is now proceeding.

## 5. Conclusions

In this study, we prepared poly(HBA/HNA) and poly(HBA/HNA/TA/BP)s with various contents of TA (or BP) up to 0.10, and examined steady shear flow viscosity for their nematic LCs in wide shear-rate range from  $10^{-3}$  to  $10^4 \text{ s}^{-1}$ . The SHG-active nematic phase is formed from the standard poly(HBA/HNA), but the SHG activity is lost by an introduction of symmetrical TA (and BP) unit into poly(HBA/HNA) because the polymer chain loses the head–tail character. The shear-viscosity curves of nematic LCs in all these copolymers invariantly show a Newtonian plateau at lowest shear rate (region 0) in addition to three conventional regions, namely low-shear-rate and high-shear-rate shear-thinning regimes (region I and region III) and the intermediate Newtonian plateau (region II). In contrast to regions II and III where the apparent viscosity shows simply positive correlation with the molecular weight, region 0 shows the distinct dependence of the viscosities on the SHG-activity. The viscosity of the SHG active copolymer is 10 times larger than that of the SHG nonactive copolymers. This difference in the viscosity is connected to the difference in the domain size measured by the small-angle light scattering method: the domain size in the SHG-active copolymer is smaller than that in the

non SHG-active copolymer. The small size of domains in the SHG-active nematic LC may be caused by its polar structure because the polar symmetry does not allow the simple annihilation for disclinations with respect to the director orientation which has been produced primarily in the powder sample.

## References and Notes

- (1) Sawyer, L. C.; Linstid, H. C.; Romer, M. *Plast. Eng. (N.Y.)* **1998**, *54*, 37.
- (2) Blackwell, J.; Biswas, A. In *Developments in oriented polymers-2*; Ward I. M., Ed.; Elsevier: New York, 1987; p 153.
- (3) Coulter, P.; Windle, A. H. *Macromolecules* **1989**, *22*, 1129.
- (4) Jin, J.-I.; Antoun, S.; Ober, C.; Lenz, R. W. *Br. Polym. J.* **1980**, *12*, 132.
- (5) Hummel, J. P.; Flory, P. J. *Macromolecules* **1980**, *13*, 479.
- (6) Imase, T.; Kawauchi, S.; Watanabe, J. *Macromol. Theory Simul.* **2001**, *10*, 434.
- (7) Watanabe, T.; Miyata, S.; Furukawa, T.; Takezoe, H.; Nishi, T.; Migita, A.; Sone, M.; Watanabe, J. *Jpn. J. Appl. Phys.* **1996**, *35*, L505.
- (8) Koike, M.; Yen, C. C.; Yuqing, L.; Tsuchiya, H.; Tokita, M.; Kawauchi, S.; Takezoe, H.; Watanabe, J. *Macromolecules* **2007**, *40*, 2524.
- (9) Park, B.; Kinoshita, Y.; Takezoe, H.; Watanabe, J. *Jpn. J. Appl. Phys.* **1998**, *37*, L136.
- (10) Yen, C.-C.; Tokita, M.; Park, B.; Takezoe, H.; Watanabe, J. *Macromolecules* **2006**, *39*, 1313.
- (11) Yen, C.-C.; Tagushi, Y.; Tokita, M.; Watanabe, J. *Macromolecules* **2008**, *41*, 2755.
- (12) Yu, C.-J.; Yu, M.; Lee, S.-D. *Jpn. J. Appl. Phys.* **2002**, *41*, L102.
- (13) Groh, B.; Dietrich, S. *Phys. Rev. E* **1997**, *55*, 2892–2901.
- (14) Terentjev, E. M.; Osipov, M. A.; Sluckin, T. J. *J. Phys. A* **1994**, *27*, 7047–7059.
- (15) Biscarini, F.; Zannoni, C.; Chiccoli, C.; Pasini, P. *Mol. Phys.* **1991**, *73*, 439–461.
- (16) Langelean, H. C.; Gotsis, A. D. *J. Rheol.* **1996**, *40*, 107.
- (17) Gotsis, A. D.; Baird, D. G. *J. Rheol.* **1985**, *29*, 539.
- (18) Onogi, S.; Asada, T. In *Proceedings of the VIIIth International Congress on Rheology*; Astarita, G.; Marrucci, G.; Nicolais, L., Eds.; Plenum: New York, 1980; pp 127–147.
- (19) Romo-Uribe, A.; Windle, A. H. *Macromolecules* **1996**, *29*, 6246.
- (20) Kromer, H.; Khun, R.; Pielartzik, H.; Siebke, W.; Eckhardt, V.; Schmidt, M. *Macromolecules* **1991**, *24*, 1950.
- (21) Calundann, G. US 4,161,470, **1979**.
- (22) Viney, C.; Donald, A. M.; Windle, A. H. *J. Mater. Sci.* **1983**, *18*, 1136.
- (23) Langellan, H. C.; Gotsis, A. D. *J. Rheol.* **1996**, *40*, 107.
- (24) Sigillo, I.; Grizzuti, N. *J. Rheol.* **1994**, *38*, 589.
- (25) Wissbrum, K. J. *J. Rheol.* **1981**, *25*, 619.
- (26) Kim, K. M.; Cho, H.; Chung, I. J. *J. Rheol.* **1994**, *38*, 1271.
- (27) Larson, R. G.; Doi, M. J. *J. Rheol.* **1991**, *35*, 539.
- (28) Hashimoto, T.; Nakai, A.; Shiwa, T.; Hasegawa, H.; Rojstaczer, S.; Stein, R. S. *Macromolecules* **1989**, *22*, 422.
- (29) Malkin, A. Y.; Masalova, I.; Slatter, P.; Wilson, K. *Rheol. Acta* **2004**, *43*, 584.
- (30) Shiwa, T.; Nakai, A.; Wang, W.; Hasegawa, H.; Hashimoto, T. *Liquid Cryst.* **1995**, *19*, 679.
- (31) Saupe, A. *Mol. Cryst. Liq. Cryst.* **1973**, *21*, 211.
- (32) Kleman, M. *Points, Lines and Walls. In Liquid Crystals, Magentic Systems, and Various Ordered Media*; Wiley: Chichester, U.K., 1983.
- (33) Rey, A. D.; Tsuji, T. *Macromol. Theory Simul.* **1998**, *7*, 623.

MA802736U